Electromagnetic transition form factors of the Roper resonance in effective field theory

T. Bauer,[1] S. Scherer,[1] and L. Tiator[1]

[1]*PRISMA Cluster of Excellence, Institut für Kernphysik, Johannes Gutenberg-Universität Mainz, D-55099 Mainz, Germany*

(Dated: February 4, 2014)

Abstract

We analyze the form factors of the electromagnetic nucleon-to-Roper-resonance transition in the framework of low-energy effective field theory. A systematic power-counting procedure is generated by applying the complex-mass scheme. Within this power counting we calculate the form factors to next-to-next-to-leading order and fit the results to empirical data.

PACS numbers: 12.39.Fe, 13.40.Gp, 14.20.Gk

arXiv:1402.0741v1 [nucl-th] 4 Feb 2014

I. INTRODUCTION

In order to explore the structure of the nucleon and its excitations a substantial experimental effort has been made to measure pion photo- and electroproduction at electron accelerators such as Bates, ELSA, JLab, and MAMI. Analyzing the available electroproduction data, transition form factors for all four-star resonances below center-of-mass energies of two GeV have been extracted in the framework of phenomenological models (see, e.g., Refs. [1–4] for an overview). Knowledge about the transition form factors is necessary to obtain a complete understanding of the nucleon excitation spectrum. In that context, precise data over a wide range of momentum transfers have also been extracted for the $P_{11}(1440)$ transition form factors [5–10]. The $P_{11}(1440)$ resonance, often referred to as Roper resonance, is the first excited state of the nucleon with quantum numbers $I(J^P) = \frac{1}{2}(\frac{1}{2}^+)$ [11]. The Q^2 dependence of the measured nucleon-to-Roper helicity amplitudes supports the simple quark model assumption that it constitutes the first radial excitation of the nucleon [9, 12]. On the other hand, describing the Roper resonance in the framework of the simplest spherically symmetric constituent quark model with SU(6) spin-flavor symmetry leads to a parity reversal pattern since, in contrast to the quark model calculations, the $S_{11}(1535)$ turns out to be heavier than the Roper resonance [13, 14]. By applying QCD-inspired potentials, the right level ordering between the two resonances can be generated within relativistic quark models [15]. Further understanding of the nature of the Roper resonance and the level ordering is provided by lattice QCD. After also observing the wrong parity reversal pattern in early studies [16–18], recent numerical simulations on the lattice hint towards the correct level ordering [19–24].

Theoretical studies of the transverse and scalar (longitudinal) helicity amplitudes have been performed in various frameworks such as nonrelativistic constituent quark models (including relativistic corrections) [25–27], relativistic quark models [28–31], chiral quark models [32–34], different hybrid models [35, 36], approaches including vector-meson-dominance features [37, 38], and lattice QCD [39, 40]. Even though the empirical data for the transverse and scalar (longitudinal) helicity amplitudes can be described fairly well for larger values of the squared momentum transfer in the framework of relativistic quark models as well as in lattice QCD, neither of the two approaches predicts the behavior in the low-Q^2 region correctly [9, 12, 29, 33, 37, 39, 40]. The aim of this article is to investigate the electromagnetic nucleon-to-Roper-resonance transition form factors in the framework of low-energy effective field theory (EFT) which is based on chiral perturbation theory [41, 42] (see, e.g., Refs. [43, 44] for an introduction). Considering only the Goldstone boson sector of QCD, within this approach a straightforward power counting, i.e., correspondence between the loop expansion and the chiral expansion in terms of momenta and quark masses at a fixed ratio [42], is obtained by using dimensional regularization in combination with a minimal subtraction scheme. The construction of a consistent power counting in effective field theories with heavy degrees of freedom turns out to be a more complex problem [45] which can be resolved by choosing a suitable renormalization scheme [46–50]. In order to also include resonant degrees of freedom, such as the Roper resonance, we apply the complex-mass scheme (CMS) [51–55], an extension of the on-mass-shell renormalization scheme to unstable particles. In the context of the strong interaction, the CMS has successfully been used to calculate the pole masses and widths of the ρ meson [56] and the Roper resonance [57]. Furthermore, electromagnetic properties have been investigated such as the magnetic moments of the Roper resonance [58] and the ρ meson [59] as well as the pion vector form

factor in the timelike region [60]. Finally, the CMS was shown to respect unitarity in a perturbative framework [61].

This article is organized as follows. In Sec. II, we briefly discuss the effective Lagrangians on which the subsequent calculation is based. The applied renormalization scheme and the power-counting rules are described in Sec. III. In Sec. IV, we give a definition of the electromagnetic transition form factors as well as the corresponding helicity amplitudes. In Sec. V, we discuss the fit of our results to empirical data and analyze our final results. Section VI contains a short summary.

II. EFFECTIVE LAGRANGIAN

In this section, we specify the effective Lagrangian relevant for the subsequent calculation of the transition form factors of the Roper resonance at next-to-next-to-leading order (NNLO). Besides the pion, the nucleon, and the Roper resonance, we also include the ρ meson as an explicit degree of freedom. The effects of other resonances such as the delta resonance are parametrized in low-energy coupling constants. As is well known from calculations of the electromagnetic form factors of the nucleon [62–64] and the Δ-resonance transition form factors [65], the explicit inclusion of the ρ meson is essential for generating sufficient curvature in the theoretically predicted results.

We write the effective Lagrangian as[1]

$$\mathcal{L}_{\rm EFT} = \mathcal{L}_\pi + \mathcal{L}_0 + \mathcal{L}_{NR} + \mathcal{L}_\rho\,, \tag{1}$$

where $\mathcal{L}_\pi$ denotes the lowest-order Goldstone-boson Lagrangian including the quark-mass term and the interaction with the external electromagnetic four-vector potential $\mathcal{A}_\mu$ [44]:

$$\mathcal{L}_\pi = \frac{F^2}{4}{\rm Tr}\left(\partial_\mu U \partial^\mu U^\dagger\right) + \frac{F^2 M^2}{4}{\rm Tr}\left(U^\dagger + U\right) + i\,\frac{F^2}{2}{\rm Tr}\left[\left(\partial^\mu U U^\dagger + \partial^\mu U^\dagger U\right) v_\mu\right]. \tag{2}$$

The pion fields are contained in the unimodular, unitary, (2×2) matrix U:

$$U(x) = u^2(x) = \exp\left(i\frac{\phi(x)}{F}\right), \quad \phi = \phi_k \tau_k.$$

The external electromagnetic four-vector potential $\mathcal{A}_\mu$ enters into $v_\mu = -e\,\mathcal{A}_\mu \tau_3/2$ [$e^2/(4\pi) \approx 1/137, e>0$]. F denotes the pion-decay constant in the chiral limit, $F_\pi = F[1+O(\hat m)] = 92.2$ MeV, and M is the pion mass at leading order in the quark-mass expansion: $M^2 = 2B\hat m$, where B is related to the quark condensate $\langle\bar q q\rangle_0$ in the chiral limit [42].

Introducing nucleon and Roper-resonance isospin doublets, N and R, with bare masses m_{N0} and m_{R0}, respectively, $\mathcal{L}_0$ reads

$$\mathcal{L}_0 = \bar N\left(i\not{D} - m_{N0} + \frac{\mathsf{g}_A}{2}\gamma^\mu\gamma_5 u_\mu\right)N + \bar R\left(i\not{D} - m_{R0} + \frac{g_R}{2}\gamma^\mu\gamma_5 u_\mu\right)R, \tag{3}$$

where g_A corresponds to the chiral limit of the axial-vector coupling constant, $g_A = 1.2701(25)$ [66], and g_R represents the analogue for the Roper-resonance case. The building block u_μ is given by

$$u_\mu = i\left[u^\dagger\partial_\mu u - u\partial_\mu u^\dagger - i\,\left(u^\dagger v_\mu u - u v_\mu u^\dagger\right)\right], \tag{4}$$

[1] To simplify the notation, only bare masses are supplied with a subscript 0.

and the covariant derivatives are defined as

$$\begin{aligned} D_\mu H &= \left(\partial_\mu + \Gamma_\mu - i\, v_\mu^{(s)}\right) H, \\ \Gamma_\mu &= \frac{1}{2}\left[u^\dagger \partial_\mu u + u \partial_\mu u^\dagger - i\left(u^\dagger v_\mu u + u v_\mu u^\dagger\right)\right], \end{aligned} \tag{5}$$

where H stands for either the nucleon or the Roper resonance and $v_\mu^{(s)} = -e\mathcal{A}_\mu/2$. By expanding u_μ of Eq. (4) for $v_\mu = 0$ in terms of the pion fields, one obtains from Eq. (3) the Goldberger-Treiman relation $\mathtt{g}_{\pi NN} = m\,\mathtt{g}_A/F$ [67, 68], where $\mathtt{g}_{\pi NN}$ and m denote the chiral limit of the pion-nucleon coupling constant and the nucleon mass, respectively. An analogous relation results for the Roper resonance.

The interaction terms $\mathcal{L}_{NR}$ are constructed in accordance with Ref. [69]. The leading-order interaction between the nucleon and the Roper is given by

$$\mathcal{L}_{NR}^{(1)} = \frac{g_{NR}}{2}\,\bar{R}\gamma^\mu\gamma_5 u_\mu N + \text{H.c.}, \tag{6}$$

where H.c. refers to the Hermitian conjugate and g_{NR} is an unknown coupling constant. The second- and third-order Lagrangians for the nucleon-Roper-resonance interaction relevant for our calculation read

$$\begin{aligned} \mathcal{L}_{NR}^{(2)} &= \bar{R}\left[\frac{c_6^*}{2}\, f_{\mu\nu}^+ + \frac{c_7^*}{2}\, v_{\mu\nu}^{(s)}\right]\sigma^{\mu\nu} N + \text{H.c.} + \cdots, \\ \mathcal{L}_{NR}^{(3)} &= \frac{i}{2}\, d_6^* \bar{R}\left[D^\mu, f_{\mu\nu}^+\right]\, D^\nu N + \text{H.c.} + 2\, i\, d_7^* \bar{R}\left(\partial^\mu v_{\mu\nu}^{(s)}\right) D^\nu N + \text{H.c.} + \cdots, \end{aligned} \tag{7}$$

where

$$\begin{aligned} v_{\mu\nu}^{(s)} &= \partial_\mu v_\nu^{(s)} - \partial_\nu v_\mu^{(s)}, \\ f_{\mu\nu}^+ &= u f_{\mu\nu} u^\dagger + u^\dagger f_{\mu\nu} u, \\ f_{\mu\nu} &= \partial_\mu v_\nu - \partial_\nu v_\mu - i[v_\mu, v_\nu]. \end{aligned} \tag{8}$$

The coupling constants c_6^* and c_7^* are related to the isovector and isoscalar transition magnetic moments. Furthermore, the coupling constants d_6^* and d_7^* contribute to the slopes of the isovector and isoscalar transition form factors to be discussed below. As discussed in Ref. [69], interaction terms of the form

$$i\lambda_1 \bar{R} \not{D} N - \lambda_2 \bar{R} N + \text{H.c.} \tag{9}$$

need not be considered. The first term and its Hermitian conjugate can be eliminated in terms of a field transformation [70] (equation-of-motion argument). After diagonalizing the nucleon-Roper mass matrix, the effects of the λ_i terms of Eq. (9) can be absorbed in the couplings of already existing terms or higher-order terms.

Finally, we need the Lagrangian containing the ρ meson. The ρ-meson triplet consists of a pair of charged fields, $\rho_\mu^\pm = (\rho_{1\mu} \mp i\rho_{2\mu})/\sqrt{2}$, and a third neutral field, $\rho_\mu^0 = \rho_{3\mu}$. There are different approaches to include vector mesons systematically into the effective Lagrangian (see, e.g., Ref. [71]). We choose the ρ meson to transform inhomogeneously under chiral transformations (V_L, V_R),

$$\rho_\mu \mapsto K\rho_\mu K^\dagger - \frac{i}{g}\partial_\mu K K^\dagger, \tag{10}$$

where

$$\begin{aligned} \rho_\mu &= \rho_{k\mu}\frac{\tau_k}{2}, \\ K(V_L, V_R, U) &= \sqrt{V_R U V_L^\dagger}^{-1} V_R \sqrt{U}, \end{aligned} \tag{11}$$

and g is a coupling constant to be discussed below. The relevant part of the effective Lagrangian containing the ρ meson can be written as

$$\mathcal{L}_\rho = \mathcal{L}_{\pi\rho} + \mathcal{L}_{\pi\rho N} + \mathcal{L}_{\pi\rho R} + \mathcal{L}_{\pi\rho NR}. \tag{12}$$

The part describing the ρ meson and its interaction with pions reads [64, 71]

$$\mathcal{L}_\rho = -\frac{1}{2}\mathrm{Tr}\left(\rho_{\mu\nu}\rho^{\mu\nu}\right) + M_{\rho 0}^2 \mathrm{Tr}\left[\left(\rho_\mu - \frac{i}{g}\Gamma_\mu\right)\left(\rho^\mu - \frac{i}{g}\Gamma^\mu\right)\right] + \cdots, \tag{13}$$

where

$$\rho_{\mu\nu} = \partial_\mu\rho_\nu - \partial_\nu\rho_\mu - ig[\rho_\mu, \rho_\nu],$$

and $M_{\rho 0}$ denotes the (bare) ρ-meson mass. Note that the structure proportional to the low-energy constant (LEC) d_x of Ref. [64] does not contribute to the *transition* form factors at NNLO and is, therefore, omitted from Eq. (13). The coupling constant g can be fixed via the Kawarabayashi-Suzuki-Riazuddin-Fayyazuddin relation [72, 73],

$$M_\rho^2 = 2g^2F^2, \tag{14}$$

generated by the combination of chiral symmetry and the consistency of the EFT with respect to renormalizability [74]. Equation (13) is self-consistent with respect to constraints and perturbative renormalizability [75].

The remaining parts of the Lagrangian relevant for the subsequent calculation are given by

$$\begin{aligned} \mathcal{L}_{\pi\rho N} &= \bar{N}\left[k_1\left(\rho_\mu - \frac{i}{g}\Gamma_\mu\right)\gamma^\mu\right]N + \cdots, \\ \mathcal{L}_{\pi\rho R} &= \bar{R}\left[k_2\left(\rho_\mu - \frac{i}{g}\Gamma_\mu\right)\gamma^\mu\right]R + \cdots, \\ \mathcal{L}_{\pi\rho NR} &= \bar{R}\left[\frac{k_3}{2}\rho_{\mu\nu}\sigma^{\mu\nu} + k_4\left[D^\mu, \rho_{\mu\nu}\right]D^\nu\right]N + \mathrm{H.c.} + \cdots. \end{aligned} \tag{15}$$

In the following, we assume that the ρ meson couples universally, meaning that the self-coupling of the ρ meson equals the coupling of the ρ meson to pions and nucleons, $k_1 = g$. Moreover, we also assume that the ρ meson couples universally to the Roper resonance, i.e., $k_2 = g$. These universality conditions are supposed to be a consequence of consistency conditions imposed by the demand of perturbative renormalizability [74].

III. RENORMALIZATION AND POWER COUNTING

In the following, we apply the CMS which originally was developed in the context of the Standard Model to derive properties of $W^{\pm}$, Z^0, and Higgs bosons obtained from resonant processes [51–55]. In Refs. [56–59], the renormalization prescriptions were modified to obtain a consistent power counting in the framework of EFT. Referring to these articles, we split the bare parameters (and fields) of the Lagrangian into, in general, complex renormalized parameters and counter terms. We choose the renormalized masses as the poles of the dressed propagators in the chiral limit:

$$\begin{aligned} m_{R0} &= z_\chi + \delta z_\chi \,, \\ m_{N0} &= m + \delta m \,, \\ M_{\rho 0} &= M_{\rho\chi} + \delta M_{\rho\chi} \,, \end{aligned} \tag{16}$$

where z_χ is the complex pole of the Roper propagator in the chiral limit, m is the mass of the nucleon in the chiral limit, and $M_{\rho\chi}$ is the complex pole of the ρ-meson propagator in the chiral limit. We include the renormalized parameters z_χ, m, and $M_{\rho\chi}$ in the propagators and treat the counter terms perturbatively. The renormalized couplings are chosen such that the corresponding counter terms exactly cancel the power-counting-violating parts of the loop diagrams.

Since the starting point is a Hermitian Lagrangian in terms of bare parameters and fields unitarity cannot be violated in the complete theory. Generalizing the notion of cutting rules [76] to unstable particles, in Ref. [61] it was shown at the one-loop level that within the CMS unitarity is also satisfied in a perturbative sense. In this context, it has been verified that unstable particles do not appear as asymptotic states and are therefore excluded from the unitarity condition [77].

We organize our perturbative calculation by applying the standard power counting of Refs. [78, 79] to the renormalized diagrams, i.e., an interaction vertex obtained from an $O(q^n)$ Lagrangian counts as low-energy order q^n, a pion propagator as order q^{-2}, a nucleon propagator as order q^{-1}, and the integration of a loop as order q^4. In addition, we assign the order q^{-1} to the Roper propagator and the order q^0 to the ρ-meson propagator. In practice, we implement this scheme by subtracting the loop diagrams at, in general, complex "on-mass-shell" points in the chiral limit. Since the virtual-photon four-momentum transfer q^μ counts as $O(q)$, we also assign the order q^1 to the mass difference between the Roper resonance and the nucleon.

IV. ELECTROMAGNETIC TRANSITION FORM FACTORS

The Roper resonance does not appear in the spectrum of asymptotic states as it is an unstable particle. To define the matrix element for the electromagnetic transition from the nucleon to the Roper resonance, we consider the pion electroproduction amplitude for an invariant energy near the mass of the Roper resonance. For the incoming nucleon, being a stable particle, on-shell kinematics correspond to $p_i^2 = m_N^2$. On the other hand, for unstable particles such as the outgoing Roper resonance, the analogous kinematical point is given by the pole position, i.e., $p_f^2 = z^2$. Introducing "Dirac spinors" $\bar{w}^i$ and w^j with complex masses z for the final lines, in Ref. [80] the authors described a method how to extract from the general vertex only those pieces which survive at the pole. The renormalized vertex function

for $p_i^2 = m_N^2$ and $p_f^2 = z^2$ may be written in terms of two transition form factors,[2]

$$\sqrt{Z_R}\,\bar{w}^i(p_f)\Gamma^\mu(p_f,p_i)u^j(p_i)\sqrt{Z_N} = \bar{w}^i(p_f)\left[\left(\gamma^\mu - \not{q}\frac{q^\mu}{q^2}\right)\tilde{F}_1^*(Q^2) + \frac{i\sigma^{\mu\nu}q_\nu}{M_R+m_N}\tilde{F}_2^*(Q^2)\right]u^j(p_i), \tag{17}$$

where Z_R and Z_N are the residues of the dressed propagators of the Roper resonance and the nucleon, respectively. Moreover, we introduced the positive-valued quantity $Q^2 = -q^2 = -(p_f - p_i)^2$. The normalization of the Pauli form factor $\tilde{F}_2^*$ features the sum of the nucleon mass m_N and the Breit-Wigner mass of the Roper resonance $M_R = 1.44$ GeV. We choose this normalization to improve comparability of our results with phenomenological analyses. Both transition form factors are complex-valued functions even for $q^2 < 0$ because of the resonance character of the Roper. In contrast to the elastic case, the coefficient of the Dirac form factor $\tilde{F}_1^*$ contains a term proportional to q^μ so that current conservation can be fulfilled. It is common to parametrize the nucleon-to-Roper transition in terms of the transverse and scalar (longitudinal) helicity amplitudes $A_{1/2}$ and $S_{1/2}$, respectively, defined in the rest frame of the Roper resonance. The relation between the helicity amplitudes extracted from experimental data and the matrix elements of the current operator defines the coupling only up to a phase, which in the present context reduces to a sign $\zeta = \pm 1$ [1, 3, 81]. We therefore define

$$F_i^*(Q^2) = \zeta\tilde{F}_i^*(Q^2). \tag{18}$$

With this convention, the transverse and scalar (longitudinal) helicity amplitudes can be expressed as the following linear combinations of the form factors F_1^* and F_2^* [8]:

$$\begin{aligned} A_{1/2}(Q^2) &= \frac{e\,Q_-}{\sqrt{4Km_NM_R}}\Big(F_1^*(Q^2) + F_2^*(Q^2)\Big), \\ S_{1/2}(Q^2) &= \frac{e\,Q_-}{\sqrt{8Km_NM_R}}\left(\frac{Q_-Q_+}{2M_R}\right)\frac{M_R+m_N}{Q^2}\left[F_1^*(Q^2) - \frac{Q^2}{(M_R+m_N)^2}F_2^*(Q^2)\right], \end{aligned} \tag{19}$$

with

$$\begin{aligned} K &= \frac{M_R^2 - m_N^2}{2M_R}, \\ Q_\pm &= \sqrt{(M_R \pm m_N)^2 + Q^2}. \end{aligned}$$

According to [1, 3, 81], in Eq. (18) we choose $\zeta = -1$ if $g_{\pi NN}$ and $g_{\pi NR}$ have the same sign and $\zeta = 1$ for opposite signs. In the present context, this translates into comparing the signs of g_A and g_{NR}.

At NNLO [$O(q^3)$], the vertex function $\Gamma^\mu(p_f,p_i)$ obtains contributions from four tree diagrams (see Fig. 1) and eighteen loop diagrams (see Fig. 2). According to Eq. (15), there is no nucleon-photon-Roper and no nucleon-ρ-Roper interaction at $O(q)$. Writing the wave function renormalization constant as

$$Z_{N/R} = 1 + \delta Z_{N/R}, \tag{20}$$

[2] The tilde symbol denotes the phase convention of the present theoretical calculation.

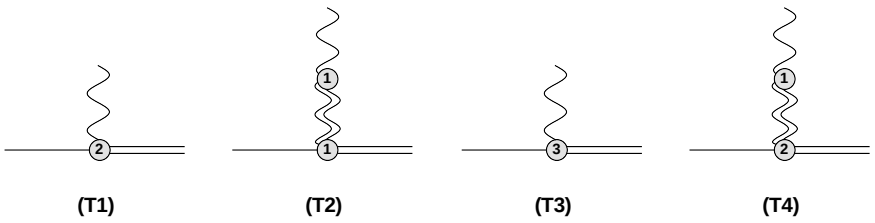


FIG. 1: Tree diagrams contributing to the electromagnetic transition form factors of the Roper resonance. Solid and wiggly lines correspond to the nucleon and the external electromagnetic field, respectively; double-solid lines correspond to the Roper and double-wiggly lines to the ρ meson. The numbers in the vertices indicate the respective orders.

TABLE I: Physical values of the parameters, where the masses and F_π are given in units of GeV and g_A is dimensionless. The values are taken from Ref. [66].

m_N	M_π	z	M_ρ	F_π	g_A
0.938	0.140	$1.365 - \frac{i}{2}\,0.190$	$0.775 - \frac{i}{2}\,0.149$	0.0922	1.27

where $\delta Z_{N/R}$ is of $O(q^2)$, we find that the product of tree diagrams (T1) and (T2) (see Fig. 1) and $\delta Z_{N/R}$ is at least of $O(q^4)$, i.e., beyond the accuracy of our calculation.

To renormalize the diagrams of Fig. 2 we first apply the modified minimal subtraction scheme of ChPT ($\widetilde{\text{MS}}$) [45]. Then, we perform additional finite subtractions such that the renormalized diagrams satisfy the given power counting. We find that the $\widetilde{\text{MS}}$-subtracted contributions to F_1^* do not contain any power-counting-violating terms. On the other hand, all power-counting-violating terms of F_2^* are analytic in small quantities and can be absorbed by the renormalization of the available coupling constants. This finding, together with current conservation, provides an important consistency check for our calculation.

V. NUMERICAL EVALUATION AND RESULTS

For the numerical evaluation of the one-loop integrals we substitute the physical values for the relevant parameters given in Table I. The difference between the physical values and the respective values in the chiral limit is beyond the given precision with respect to a (chiral) low-energy expansion. More specifically, we need to evaluate scalar one-, two-, and three-point functions with complex parameters.[3] While it is well known how to analytically continue scalar one- and two-point functions to complex internal masses and complex external invariant momenta, the evaluation of three-point functions with complex parameters is more involved and, to the best of our knowledge, only possible for a few special cases (see Ref. [83]). In order to avoid this complication, we drop the finite imaginary part of the internal masses of the Roper resonance in all loop integrals. Neglecting the imaginary part in the one-loop integrals constitutes an effect of $\mathcal{O}(\hbar^2)$ which is beyond the accuracy of our

[3] A definition of scalar loop integrals can be found in Ref. [82].

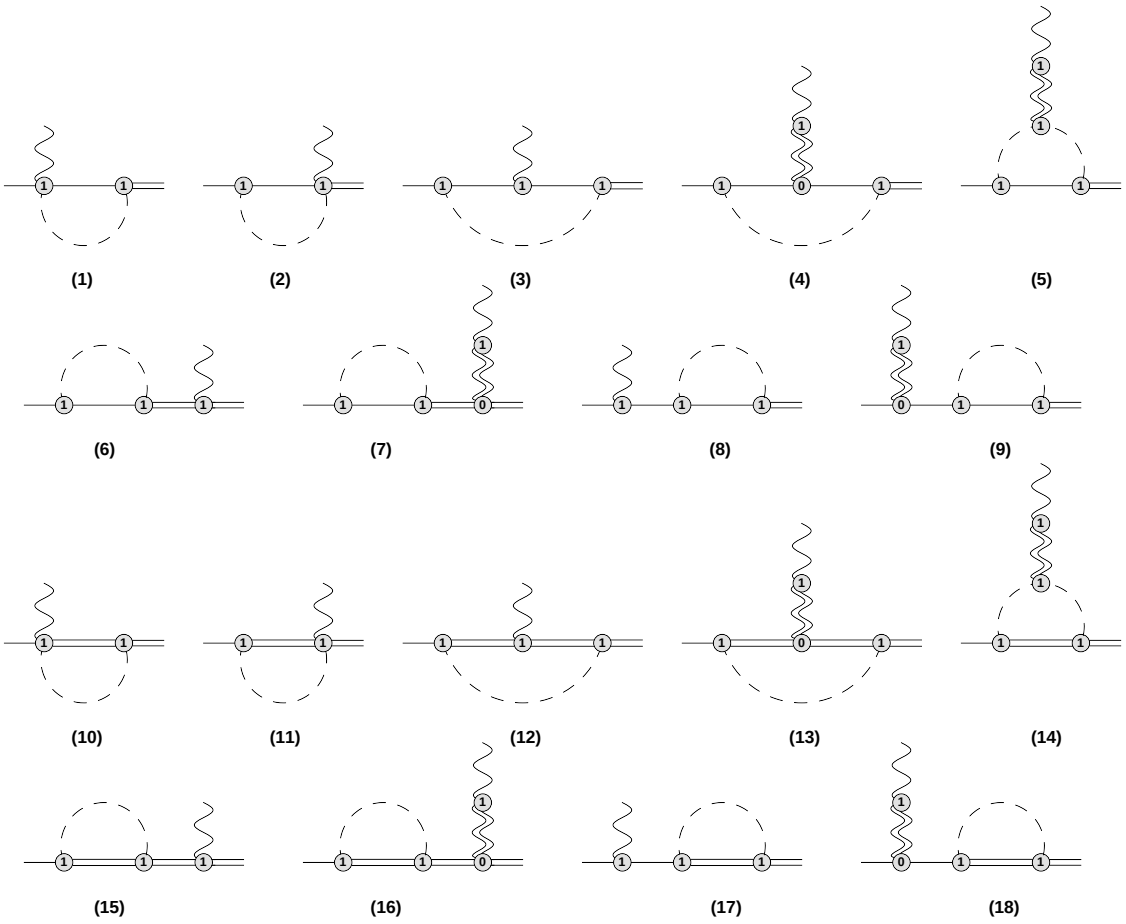


FIG. 2: Loop diagrams contributing to the electromagnetic transition form factors of the Roper resonance. Dashed, solid, and wiggly lines correspond to the pion, nucleon, and external electromagnetic field, respectively; double-solid lines correspond to the Roper and double-wiggly lines to the ρ meson. The numbers in the vertices indicate the respective orders.

one-loop calculation.

As far as the remaining eight LECs are concerned we make use of the following strategy. The couplings g_A, g_{NR}, and g_R appear in the one-loop diagrams of Fig. 2, namely, in terms of the products $\mathsf{g}_A \cdot g_{NR}$ and $g_R \cdot g_{NR}$ in diagrams (1)-(9) and (10)-(18), respectively. In order to keep the number of free parameters as small as possible, we follow Ref. [69] and take $g_R = 1$ such that g_A and g_R are roughly of the same size (the naive quark model predicts $g_A = g_R$). Furthermore, we explore the values of g_{NR} in a region of $0.1 - 0.4$, but use in our final result $g_{NR} = 0.35$ [69], compatible with a fit to the branching ratio of the Roper resonance into πN.

The remaining six parameters appear only in the tree diagrams and can be determined by a fit to data. In total, four helicity amplitudes can be analyzed from electroproduction experiments, tranverse (${}_pA_{1/2}(Q^2)$, ${}_nA_{1/2}(Q^2)$) and scalar (longitudinal) (${}_pS_{1/2}(Q^2)$, ${}_nS_{1/2}(Q^2)$) helicity amplitudes of proton and neutron, respectively. From mainly JLab experiments measured by the CLAS collaboration, analyzed helicity amplitude data are found in the literature from a MAID analysis, Ref. [8], and a CLAS analysis, Ref. [9], both from single-pion electroproduction, and from a recent CLAS analysis, Ref. [10], from two-pion electroproduc-

tion. These data points are only for a proton target and $Q^2 \geq 0.28$ GeV^2. No single-Q^2 data have yet been analyzed for the neutron target. At $Q^2 = 0$, the transverse helicity amplitudes are obtained from pion photoproduction and rather precise values are found in the Particle Data Listings [66]. The scalar helicity amplitudes ${}_pS_{1/2}(0)$ and ${}_nS_{1/2}(0)$ are in general also finite, but cannot be measured in a photoproduction experiment.

The data points are obtained from reaction models describing the electroproduction cross sections. MAID is a unitary isobar model incorporating all established resonances up to 2 GeV. The resonant contributions are parametrized in terms of a Breit-Wigner ansatz and the background is given in terms of unitarized nucleon and vector-meson Born diagrams. A similar approach is used by the CLAS collaboration, including dispersion relations as an additional constraint. The application of both models allows for the extraction of so-called single-Q^2 data for the electromagnetic transition from the proton to the positively charged Roper over a wide range of momentum transfers.

Because of the above-mentioned limitations in the data, we first performed a fit of the six parameters to the empirical helicity amplitudes obtained in the analysis of MAID2007, with an update in 2008, mainly due to new electroproduction data at higher Q^2 [8]. This fit cannot describe all four helicity amplitudes simultaneously. In particular, we find different values for the coupling k_4, which only affects the scalar helicity amplitudes, when fitted to proton and neutron amplitudes separately. However, the empirical MAID fit that was found by a global fit of the MAID model to the world data base on electroproduction of proton and neutron targets, still has quite some uncertainties, especially for the scalar neutron helicity amplitude, where practically no available data was very sensitive to. As a consequence, we tried a fit to only three empirical helicity amplitudes, by excluding the scalar neutron helicity amplitude. From this analysis with the empirical helicity amplitudes we can conclude that a large isovector coupling of the ρ meson is observed with a value $k_3 \approx -5.4$ together with a small πNR coupling of $g_{NR} \approx 0.1$.

Comparing the empirical helicity amplitudes with data (see Fig. 3), a notable deviation is observed for the slope of the transverse proton helicity amplitude ${}_pA_{1/2}(Q^2)$. Therefore, we have refitted the γNR couplings for the proton c_p^*, d_p^* to the available single-Q^2 data. The results are shown in Fig. 3, where we present our results together with both the data and the empirical fit of the helicity amplitudes. In this first figure, the πNR coupling was kept fixed at $g_{NR} = 0.175$, slightly larger than in the fit to the empirical helicity amplitudes, but only half of the value found in Ref. [69]. By increasing the πNR coupling, the loop terms increase accordingly and for the value of $g_{NR} = 0.35$ we performed a second fit, see Fig. 4. In a comparison with the data points, this second fit is very similar, however, in comparison with the empirical scalar helicity amplitudes, larger deviations are observed. Referring to the already discussed fact that the scalar helicity amplitudes are based on very little experimental information, and the more realistic pion coupling, we consider this second parametrization as our basic result. Our results for the LECs are shown in Table II. In Fig. 5, the resulting curves for the transition form factors F_1^* and F_2^* are shown.

One possible approach to obtain model-independent predictions for the transition form factors are numerical simulations on the lattice. At present, calculations of the nucleon-to-Roper-resonance transition form factors are based on the quenched approximation and seem to fail for low squared momentum transfers [39, 40]. Given the manifest Lorentz covariance of our results, they may provide useful guidance for systematical extrapolations of lattice simulations to the physical value of the pion mass. A fit of our expressions to lattice data at different values for the pion mass would result in a complete theoretical prediction of the

TABLE II: Values for the fitted LECs, where $c^*_{p/n} = \frac{c^*_7}{2} \pm c^*_6$ and k_3 are given in units of GeV^{-1}, k_4 in units of GeV^{-2}, and $d^*_{p/n} = d^*_7 \pm d^*_6$ in units of GeV^{-3}. The values of g_{NR} in the second column were fixed for the two fits, see text.

g_R	g_{NR}	c^*_p	c^*_n	d^*_p	d^*_n	k_3	k_4
1.0	0.175	0.27	−0.18	0.04	0.04	−5.5	1.0
1.0	0.35	0.29	−0.18	0.04	0.1	−4.9	1.0

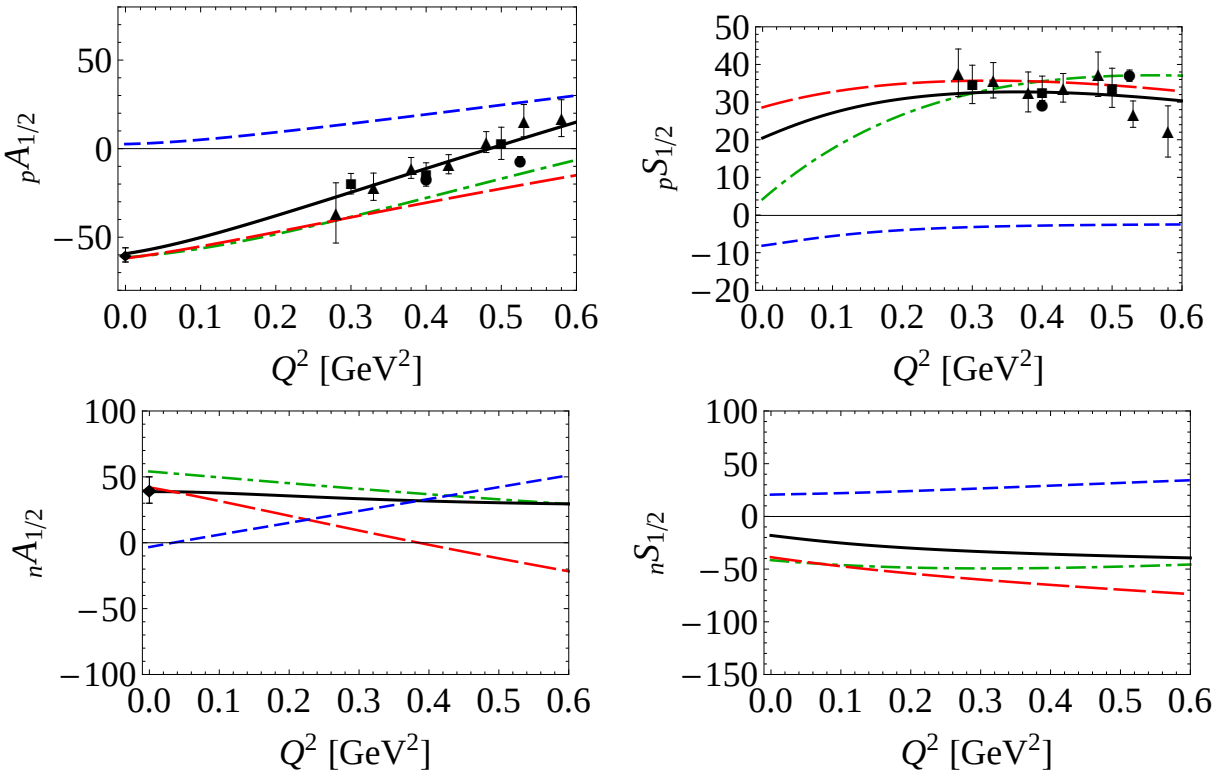


FIG. 3: (Color online) Transverse and scalar (longitudinal) helicity amplitudes $A_{1/2}$ and $S_{1/2}$ of the nucleon-to-Roper-resonance transition in units of 10^{-3} GeV$^{-1/2}$. Solid (black) lines: total results in the complex-mass scheme; long-dashed (red) lines: tree contribution; short-dashed (blue) lines: loop contribution; dash-dotted (green) lines: empirical parametrization of Ref. [8]. The data points originate from the analysis of single-pion electroproduction data (circles [6] and squares [9]) and double-pion electroproduction data (triangles [10]). The values of $A_{1/2}$ at the real-photon point are taken from Ref. [66]. The parameter values are for our fit 1, in particular, $g_{NR} = 0.175$.

transition form factors and thereby a model-independent determination of the LECs. To obtain an idea of the pion-mass dependence of the transition form factors we show F_1^* and F_2^* for different values of the pion mass in Fig. 6.

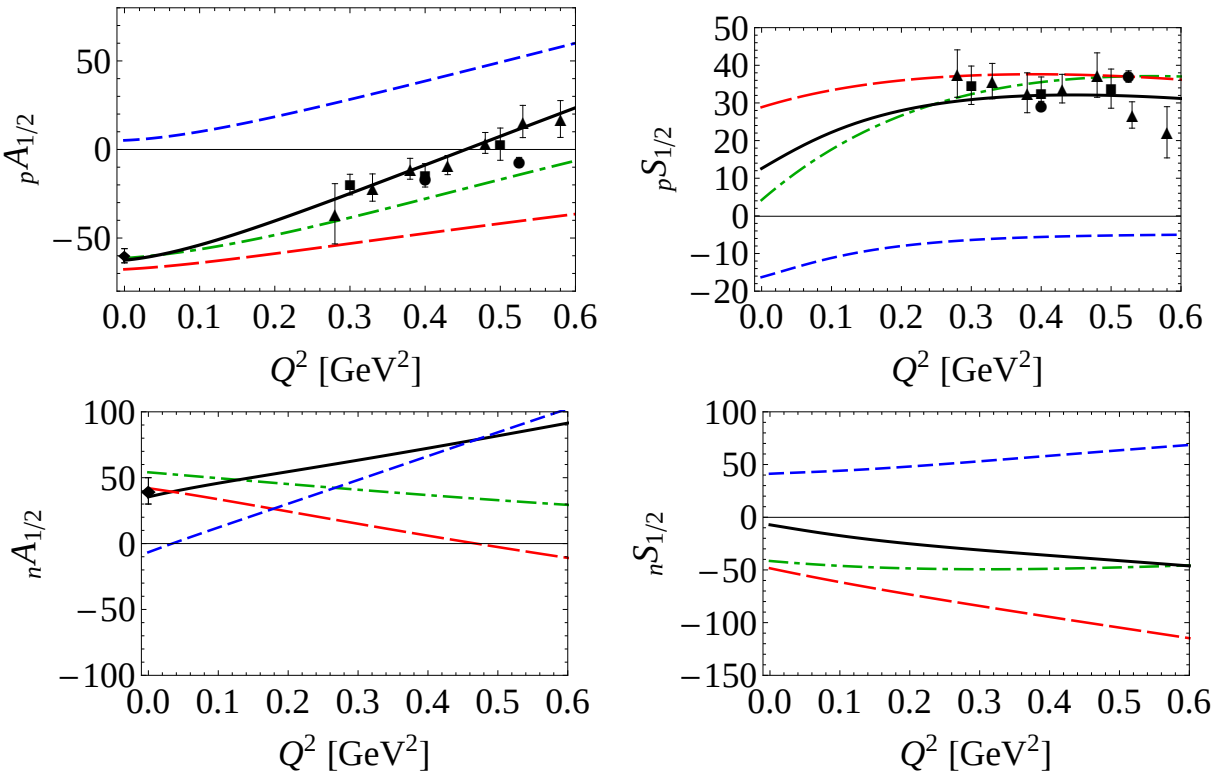


FIG. 4: (Color online) Same as in Fig. 3, except that the parameter values are for our fit 2, in particular, $g_{NR} = 0.35$.

VI. SUMMARY AND OUTLOOK

To summarize, we have calculated the electromagnetic transition form factors of the Roper resonance up to and including NNLO using EFT techniques. To obtain a systematic power counting, we applied the CMS which is a generalization of the on-mass-shell renormalization to unstable particles.

Our final results have been fitted to empirical data of the helicity amplitudes up to and including $Q^2 = 0.58$ GeV^2. Even though the obtained results are in good agreement with the empirical analyses, we stress that a one-loop calculation should be treated with care beyond $Q^2 = 0.4$ GeV^2. The reason we have extended the fits to such large values of Q^2 is the lack of empirical data in the low-Q^2 domain. In order to reduce the number of fit parameters we fixed the LECs g_R and g_{NR} since, in principle, they belong to other processes and contribute only to loop diagrams in the present calculation. The remaining six LECs were assumed to be real and determined by fitting the data of the proton helicity amplitudes and the empirical parametrization of the neutron helicity amplitudes. A potentially useful application of our calculation is in the context of lattice extrapolations. To that end, we have also discussed the pion-mass dependence of the transition form factors.

In conclusion, it is possible to systematically calculate the electromagnetic transition form factors of the Roper resonance in the framework of low-energy EFT applying the CMS and phenomenologically describe the available empirical data in the low-Q^2 region. On the other hand, due to the large difference between the nucleon and Roper resonance masses, serving as an expansion parameter, the convergence of the underlying perturbative expansion and

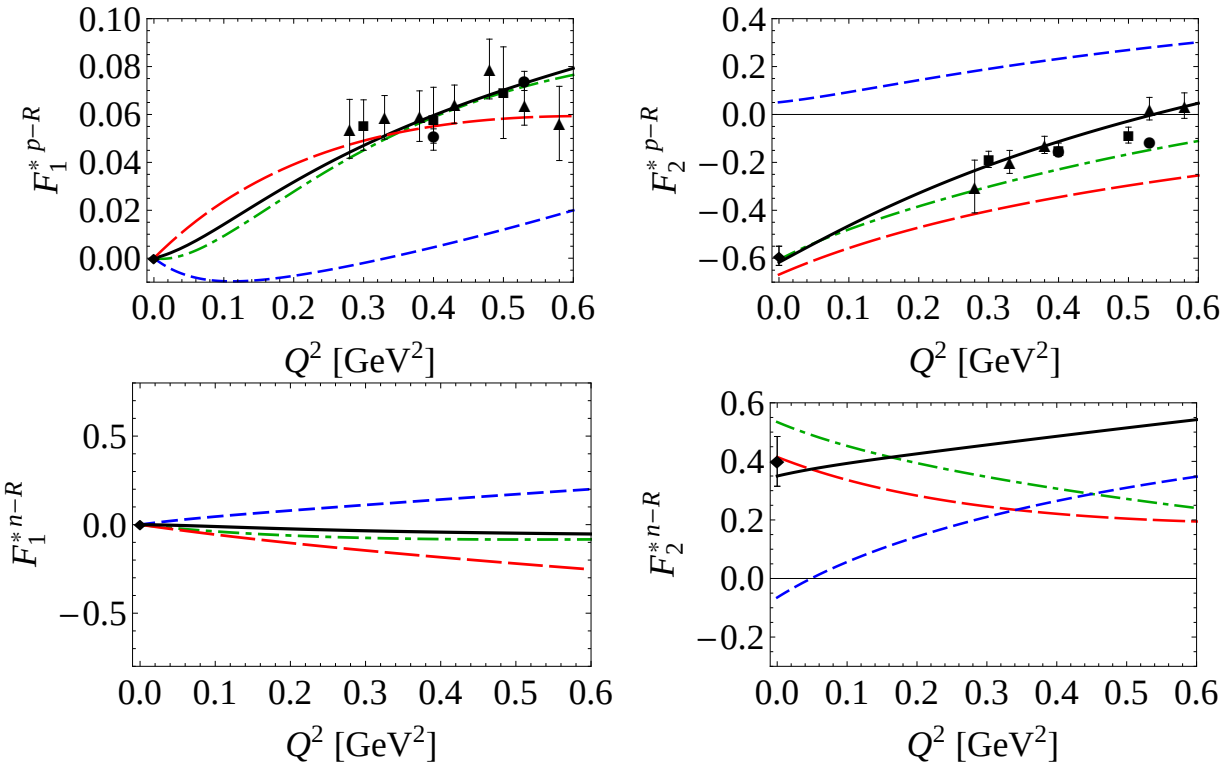


FIG. 5: (Color online) Dirac and Pauli form factors F_1^* and F_2^* of the nucleon-to-Roper-resonance transition. The meaning of the curves and of the data points as in Fig. 3. The relations between the form factors and the helicity amplitudes is given in Eq. (19). The parameter values are for our fit 2, in particular, $g_{NR} = 0.35$.

the valid region of applicability has yet to be studied more thoroughly.

The nucleon-to-Roper transition vertex containing the transition form factors appears as a building block in the resonant s channel of pion electroproduction. For this reason, a full calculation of pion electroproduction for center-of-mass energies in the region of the Roper mass seems to be feasible choosing an appropriate power counting.

Acknowledgments

When calculating the loop diagrams, we made use of the packages FeynCalc [84] and LoopTools [85]. The authors thank J. Gegelia for helpful discussions and useful comments on the manuscript. This work was supported by the Deutsche Forschungsgemeinschaft (SCHE459/4-1, SFB 443 and 1044).

[1] L. Tiator, D. Drechsel, S. S. Kamalov, and M. Vanderhaeghen, Eur. Phys. J. ST **198**, 141 (2011).
[2] I. G. Aznauryan and V. D. Burkert, Prog. Part. Nucl. Phys. **67**, 1 (2012).
[3] I. G. Aznauryan *et al.*, Int. J. Mod. Phys. E **22**, 1330015 (2013).

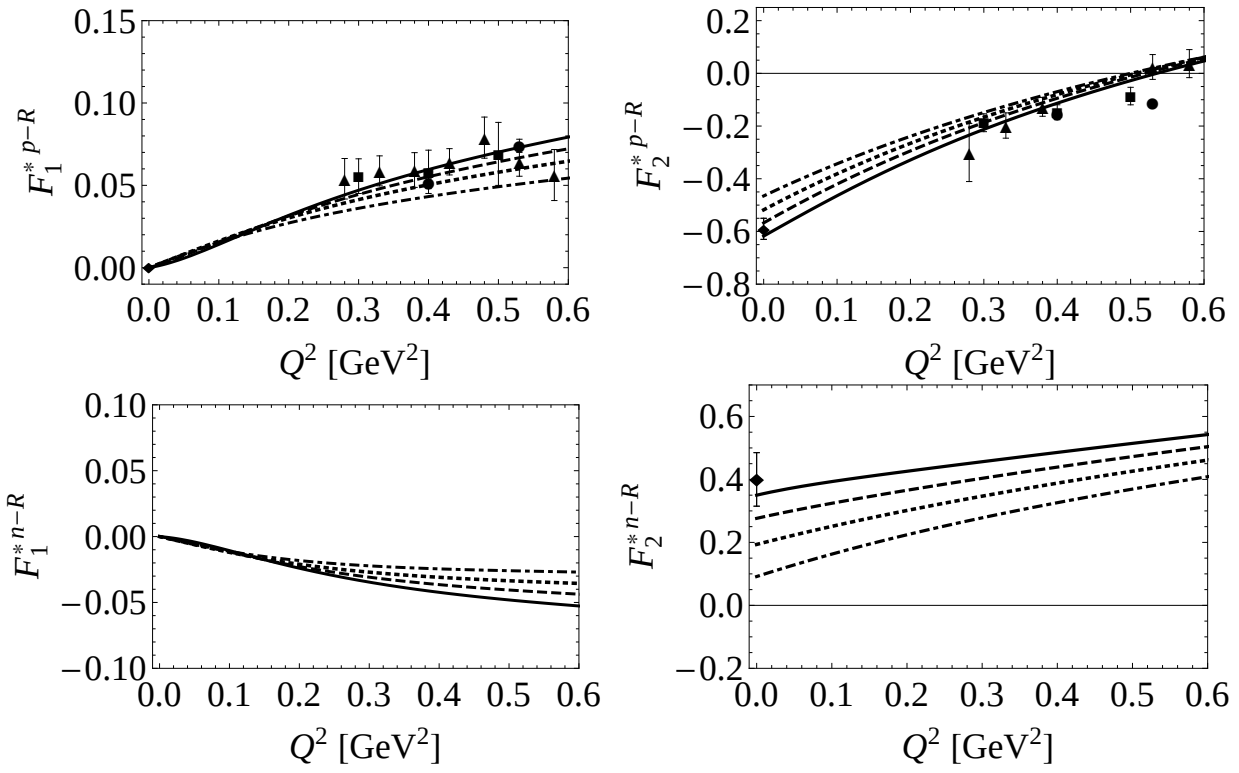


FIG. 6: Dirac and Pauli form factors F_1^* and F_2^* of the nucleon-to-Roper-resonance transition for different values of the pion mass. Solid lines refer to $M_\pi = 0.14$ GeV, dashed lines to $M_\pi = 0.2$ GeV, dotted lines to $M_\pi = 0.3$ GeV, and dash-dotted lines to $M_\pi = 0.4$ GeV, respectively. The parameter values are for our fit 2, in particular, $g_{NR} = 0.35$.

[4] V. Crede and W. Roberts, Rept. Prog. Phys. **76**, 076301 (2013).
[5] I. G. Aznauryan, V. D. Burkert, H. Egiyan, K. Joo, R. Minehart, and L. C. Smith, Phys. Rev. C **71**, 015201 (2005).
[6] D. Drechsel, S. S. Kamalov, and L. Tiator, Eur. Phys. J. A **34**, 69 (2007).
[7] I. G. Aznauryan *et al.* [CLAS Collaboration], Phys. Rev. C **78**, 045209 (2008).
[8] L. Tiator and M. Vanderhaeghen, Phys. Lett. B **672**, 344 (2009).
[9] I. G. Aznauryan *et al.* [CLAS Collaboration], Phys. Rev. C **80**, 055203 (2009).
[10] V. I. Mokeev *et al.* [CLAS Collaboration], Phys. Rev. C **86**, 035203 (2012).
[11] L. D. Roper, Phys. Rev. Lett. **12**, 340 (1964).
[12] G. Ramalho and K. Tsushima, AIP Conf. Proc. **1374**, 353 (2011).
[13] N. Isgur and G. Karl, Phys. Lett. B **72**, 109 (1977).
[14] N. Isgur and G. Karl, Phys. Rev. D **19**, 2653 (1979).
[15] L. Y. Glozman and D. O. Riska, Phys. Rept. **268**, 263 (1996).
[16] S. Sasaki, T. Blum, and S. Ohta, Phys. Rev. D **65**, 074503 (2002).
[17] W. Melnitchouk *et al.*, Phys. Rev. D **67**, 114506 (2003).
[18] R. G. Edwards *et al.* [LHP Collaboration], Nucl. Phys. Proc. Suppl. **119**, 305 (2003).
[19] F. X. Lee, S. J. Dong, T. Draper, I. Horvath, K. F. Liu, N. Mathur, and J. B. Zhang, Nucl. Phys. Proc. Suppl. **119**, 296 (2003).
[20] N. Mathur, Y. Chen, S. J. Dong, T. Draper, I. Horvath, F. X. Lee, K. F. Liu, and J. B. Zhang,

Phys. Lett. B **605**, 137 (2005).
[21] K. Sasaki, S. Sasaki, and T. Hatsuda, Phys. Lett. B **623**, 208 (2005).
[22] M. S. Mahbub, A. Ó Cais, W. Kamleh, B. G. Lasscock, D. B. Leinweber, and A. G. Williams, Phys. Lett. B **679**, 418 (2009).
[23] M. S. Mahbub, W. Kamleh, D. B. Leinweber, A. Ó Cais, and A. G. Williams, Phys. Lett. B **693**, 351 (2010).
[24] M. S. Mahbub *et al.* [CSSM Lattice Collaboration], Phys. Lett. B **707**, 389 (2012).
[25] L. A. Copley, G. Karl, and E. Obryk, Phys. Lett. B **29**, 117 (1969).
[26] S. Capstick, Phys. Rev. D **46**, 2864 (1992).
[27] E. Santopinto and M. M. Giannini, Phys. Rev. C **86**, 065202 (2012).
[28] H. J. Weber, Phys. Rev. C **41**, 2783 (1990).
[29] F. Cardarelli, E. Pace, G. Salme, and S. Simula, Phys. Lett. B **397**, 13 (1997).
[30] Y. B. Dong, K. Shimizu, A. Faessler, and A. J. Buchmann, Phys. Rev. C **60**, 035203 (1999).
[31] G. Ramalho and K. Tsushima, Phys. Rev. D **81**, 074020 (2010).
[32] K. Bermuth, D. Drechsel, L. Tiator, and J. B. Seaborn, Phys. Rev. D **37**, 89 (1988).
[33] P. Alberto, M. Fiolhais, B. Golli, and J. Marques, Phys. Lett. B **523**, 273 (2001).
[34] B. Golli, S. Sirca, and M. Fiolhais, Eur. Phys. J. A **42**, 185 (2009).
[35] Z.-p. Li, V. Burkert, and Z.-j. Li, Phys. Rev. D **46**, 70 (1992).
[36] I. T. Obukhovsky, A. Faessler, D. K. Fedorov, T. Gutsche, and V. E. Lyubovitskij, Phys. Rev. D **84**, 014004 (2011).
[37] F. Cano and P. Gonzalez, Phys. Lett. B **431**, 270 (1998).
[38] G. Vereshkov and N. Volchanskiy, Phys. Rev. D **76**, 073007 (2007).
[39] H.-W. Lin, S. D. Cohen, R. G. Edwards, and D. G. Richards, Phys. Rev. D **78**, 114508 (2008).
[40] H.-W. Lin, S. D. Cohen, R. G. Edwards, K. Orginos, and D. G. Richards, PoS LATTICE **2008**, 140 (2008).
[41] S. Weinberg, Physica A **96**, 327 (1979).
[42] J. Gasser and H. Leutwyler, Annals Phys. **158**, 142 (1984).
[43] S. Scherer, Adv. Nucl. Phys. **27**, 277 (2003).
[44] S. Scherer and M. R. Schindler, Lect. Notes Phys. **830**, 1 (2012).
[45] J. Gasser, M. E. Sainio, and A. Švarc, Nucl. Phys. B **307**, 779 (1988).
[46] H. B. Tang, arXiv:hep-ph/9607436.
[47] T. Becher and H. Leutwyler, Eur. Phys. J. C **9**, 643 (1999).
[48] J. Gegelia and G. Japaridze, Phys. Rev. D **60**, 114038 (1999).
[49] T. Fuchs, J. Gegelia, G. Japaridze, and S. Scherer, Phys. Rev. D **68**, 056005 (2003).
[50] M. R. Schindler, J. Gegelia, and S. Scherer, Phys. Lett. B **586**, 258 (2004).
[51] R. G. Stuart, in Z^0 *Physics*, ed. J. Tran Thanh Van (Editions Frontieres, Gif-sur-Yvette, 1990), p. 41.
[52] A. Denner, S. Dittmaier, M. Roth, and D. Wackeroth, Nucl. Phys. B **560**, 33 (1999).
[53] A. Denner and S. Dittmaier, Nucl. Phys. Proc. Suppl. **160**, 22 (2006).
[54] S. Actis and G. Passarino, Nucl. Phys. B **777**, 100 (2007).
[55] S. Actis, G. Passarino, C. Sturm, and S. Uccirati, Phys. Lett. B **669**, 62 (2008).
[56] D. Djukanovic, J. Gegelia, A. Keller, and S. Scherer, Phys. Lett. B **680**, 235 (2009).
[57] D. Djukanovic, J. Gegelia, and S. Scherer, Phys. Lett. B **690**, 123 (2010).
[58] T. Bauer, J. Gegelia, and S. Scherer, Phys. Lett. B **715**, 234 (2012).
[59] D. Djukanovic, E. Epelbaum, J. Gegelia, and U.-G. Meißner, arXiv:1309.3991 [hep-ph].
[60] T. Bauer, D. Djukanovic, J. Gegelia, S. Scherer, and L. Tiator, AIP Conf. Proc. **1432**, 269

(2012).
[61] T. Bauer, J. Gegelia, G. Japaridze, and S. Scherer, Int. J. Mod. Phys. A **27**, 1250178 (2012).
[62] B. Kubis and U.-G. Meißner, Nucl. Phys. A **679**, 698 (2001).
[63] M. R. Schindler, J. Gegelia, and S. Scherer, Eur. Phys. J. A **26**, 1 (2005).
[64] T. Bauer, J. C. Bernauer, and S. Scherer, Phys. Rev. C **86**, 065206 (2012).
[65] M. Hilt, T. Bauer, S. Scherer, and L. Tiator, in preparation.
[66] J. Beringer *et al.* (Particle Data Group Collaboration), Phys. Rev. D **86**, 010001 (2012).
[67] M. L. Goldberger and S. B. Treiman, Phys. Rev. **110**, 1178 (1958).
[68] Y. Nambu, Phys. Rev. Lett. **4**, 380 (1960).
[69] B. Borasoy, P. C. Bruns, U.-G. Meißner, and R. Lewis, Phys. Lett. B **641**, 294 (2006).
[70] S. Scherer and H. W. Fearing, Phys. Rev. D **52**, 6445 (1995).
[71] G. Ecker, J. Gasser, H. Leutwyler, A. Pich, and E. de Rafael, Phys. Lett. B **223**, 425 (1989).
[72] K. Kawarabayashi and M. Suzuki, Phys. Rev. Lett. **16**, 255 (1966).
[73] Riazuddin and Fayyazuddin, Phys. Rev. **147**, 1071 (1966).
[74] D. Djukanovic, M. R. Schindler, J. Gegelia, G. Japaridze, and S. Scherer, Phys. Rev. Lett. **93**, 122002 (2004).
[75] D. Djukanovic, J. Gegelia, and S. Scherer, Int. J. Mod. Phys. A **25**, 3603 (2010).
[76] R. E. Cutkosky, J. Math. Phys. **1**, 429 (1960).
[77] M. J. G. Veltman, Physica **29**, 186 (1963).
[78] S. Weinberg, Nucl. Phys. B **363**, 3 (1991).
[79] G. Ecker, Prog. Part. Nucl. Phys. **35**, 1 (1995).
[80] J. Gegelia and S. Scherer, Eur. Phys. J. A **44**, 425 (2010).
[81] I. G. Aznauryan, Phys. Rev. C **76**, 025212 (2007).
[82] A. Denner and S. Dittmaier, Nucl. Phys. B **734**, 62 (2006).
[83] G. Passarino, C. Sturm, and S. Uccirati, Nucl. Phys. B **834**, 77 (2010).
[84] R. Mertig, M. Bohm, and A. Denner, Comput. Phys. Commun. **64**, 345 (1991).
[85] T. Hahn and M. Perez-Victoria, Comput. Phys. Commun. **118**, 153 (1999).